

# POSITRON SOURCE FROM BETATRON X-RAYS EMITTED IN A PLASMA WIGGLER\*

D.K. Johnson, C.E. Clayton, C. Huang, C. Joshi, W. Lu, K.A. Marsh,  
W. Mori, M. Zhou, UCLA, Los Angeles, CA, 90095  
C.D. Barnes, F.J. Decker, M.J. Hogan, R. Iverson, P. Krejcik,  
C.O'Connell, R. Siemann, D.R. Walz, SLAC, Stanford, CA 94025, USA,  
S. Deng, T.Katsouleas, P. Muggli, E.Oz, USC, Los Angeles, CA 90089, USA

## Abstract

In the E-167 plasma wakefield accelerator (PWFA) experiments in the Final Focus Test Beam (FFTB) at the Stanford Linear Accelerator Center (SLAC), an ultra-short, 28.5 GeV electron beam field ionizes a neutral column of Lithium vapor. In the underdense regime, all plasma electrons are expelled creating an ion column. The beam electrons undergo multiple betatron oscillations leading to a large flux of broadband synchrotron radiation. With a plasma density of  $3 \times 10^{17} \text{ cm}^{-3}$ , the effective focusing gradient is near 9 MT/m with critical photon energies exceeding 50 MeV for on-axis radiation. A positron source is the initial application being explored for these X-rays, as photo-production of positrons eliminates many of the thermal stress and shock wave issues associated with traditional Bremsstrahlung sources. Photo-production of positrons has been well-studied; however, the brightness of plasma X-ray sources provides certain advantages. In this paper, we present results of the simulated radiation spectra for the E-167 experiments, and compute the expected positron yield.

## INTRODUCTION

In the E-167 experiments at SLAC, an ultra-short, 28.5 GeV electron beam field ionizes a neutral column of Li vapor. If the beam density is larger than the plasma density, plasma electrons are blown out leaving a longitudinal ion column. The ion column exerts a transverse focusing force on the beam leading to electron betatron oscillations. The electron "wiggles" are due to the radial electrostatic field of the ion column (MKS units) [1]

$$E_r = \frac{1}{2} \frac{n_{pe} e}{\epsilon_0} r \quad (1)$$

where  $n_{pe}$  is the plasma density and  $e$  is the electron charge. To compare this "plasma wiggler" to its magnetic counterparts, it is convenient to describe this electrostatic focusing force in terms of an effective magnetic field found from Eqn. (1) as

$$B_\theta / r = 3 \times 10^{-11} n_{pe} [cm^{-3}] T/m \quad (2)$$

For the E-164X experiment, a standard plasma density was  $n_{pe} = 3 \times 10^{17} \text{ cm}^{-3}$  with a beam size of  $\sigma_r = 10 \mu\text{m}$ , giving an effective focusing field of 90 T.

\* Work supported by DOE contracts DE-FG02-92ER40727 (UCLA), NSF Grants 087891 and Phy0321345., DE-AC02-76SF00515 (SLAC), and DE-FG02-92ER40745 (USC),

The following derivations in this section reference Esarey et al. [1]. All electrons within the beam undergo harmonic motion along the axis of the channel described by the betatron frequency,  $\omega_\beta = w_{pe} / \sqrt{2} \gamma$ , where  $w_{pe}$  is the electron plasma frequency and  $\gamma$  is the Lorentz factor of the beam electrons. The fundamental parameter describing all wigglers is the wiggler strength,  $K$ , defined as

$$K = \gamma k_\beta r \quad (3)$$

where  $k_\beta$  is the betatron wavenumber ( $= \omega_\beta / c$ ) and  $r$  is the radius of the oscillating electron. The spectrum of the betatron radiation has resonant frequencies defined by

$$\omega_n = \frac{n 2 \omega_\beta \gamma^2}{1 + K^2 / 2 + (\gamma \theta)^2} \quad (4)$$

where  $\theta$  is the angle between the axial motion of the beam and the observation point and  $n$  is the harmonic number. Equation (4) is completely analogous to its magnetic wiggler counterparts. The only difference being the definition of the wiggler strength.

As seen in Eqn. (3), the wiggler strength is linearly proportional to radius. This has important implications to a high  $K$  wiggler. When  $K$  is small ( $K \sim 1$ ), the spectral power is dominated by the first harmonic with a characteristic FWHM of  $1/N_\beta$ , where  $N_\beta$  is the number of betatron oscillations within the plasma. However, when  $K$  is large ( $K \gg 1$ ), higher harmonic radiation dominates, and individual electrons at different radii have different resonant frequencies resulting in a broadband spectrum. This spectrum is defined by a critical energy and critical harmonic number. For on-axis radiation ( $\theta = 0$ ), these quantities are  $\omega_c = 3K\gamma^2\omega_\beta/2$  and  $n_c = 3K^3/8$ , respectively.

The electron energy loss is found from the relativistic Larmor Formula. Using the betatron orbits due to the radial electrostatic potential, the energy loss per unit length is

$$\frac{dW_{loss}}{dz} = \frac{1}{3} r_e m_e \gamma^2 \omega_\beta^2 K^2 \quad (5)$$

where  $m_e$  is the electron mass and  $r_e$  is the electron radius.

For a 28.5 GeV electron, with the experimental parameters listed above, we find a  $\sigma_r = 10 \mu\text{m}$  electron experiences a wiggler strength  $K = 173$  with a critical energy of roughly 49.6 MeV on-axis. This electron radiates nearly 4.3 GeV/m.

One of the purposes of this experiment is to explore whether these photons could lead to a useful positron

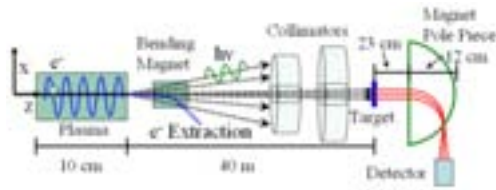


Figure 1: Experimental schematic. Not drawn to scale.

source. If the photons target on a high-Z material, they are expected to produce large amounts of electron/positron pairs. However, conversion efficiency is largely material independent when the target thickness is less than one radiation length and the photon energy is roughly 30 MeV [2]. This allows the use of a lower-Z material with a higher heat conductivity; thus, decreasing the probability of target failure. The material chosen is Ti.

## EXPERIMENTAL SETUP

Figure 1 shows the schematic for the positron experiment. The electrons radiate photons in a 10cm plasma. The photons must propagate 40 meters downstream to the target due to space limitations in the FFTB. After 40m with  $n_{pe} = 3 \times 10^{17} cm^{-3}$ , radiation exists out to a radius of 35 cm. To eliminate noise from the outermost radiation, the beam is collimated, creating an 8mm spot at the target.

The beam collides with a target resulting in pair production. The positrons are imaged using a magnetic spectrometer with an aperture of roughly 1.46cm by 5.08cm, about 23cm downstream of the target. The positrons are detected using 1mm Silicon Surface Barrier Detectors in the vertical focal plane. Positrons have been imaged up to energies of 25 MeV. In the near future, we plan to image both polarities simultaneously, and the magnetic field will be increased, allowing positron imaging to 35 MeV.

## SIMULATION OF EXPERIMENT

Plasma betatron X-rays were first observed in the E-157 experiment at SLAC [3]. The measurement of these X-rays was possible due to the relatively low experimental plasma densities ( $n_{pe} \sim 1 \times 10^{14} cm^{-3}$ ) which created a large signal between 10-20 keV. Spectra in this energy range are measured using conventional Bragg scattering. Given the broadband nature of the MeV photon source, the measurement of the absolute photon spectrum becomes difficult. Therefore, numerical methods are employed to simulate the photon spectrum that creates the pairs in the experiment.

### Spectrum Calculation

The radiation spectrum from an accelerated charged particle in a plasma wiggler has been derived, and the result gives multiple infinite Bessel Function sums [1]. At high K, the Bessel functions converge too slowly, and the number of harmonics ( $\sim K^3$ ) is too large to resolve, making

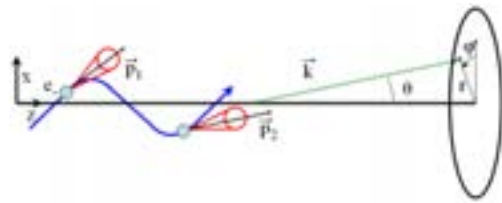


Figure 2: Saddle-Point Method schematic.  $\vec{k} \cdot \vec{p}_1$  is small, but  $\vec{k} \cdot \vec{p}_2$  is large. Thus,  $\vec{p}_2$  will have a large contribution to the spectrum along  $\vec{k}$ .

the calculation unfeasible on a single processor. An alternative method for computing the spectrum is illustrated in Figure 2. It is well-known that synchrotron radiation is emitted in a cone angle  $\theta = 1/\gamma$  around the instantaneous momentum vector ( $\vec{p}$ ) of the particle. Assuming x-z plane betatron motion, we get a characteristic divergence angle of  $\theta_y = 1/\gamma$  perpendicular to the particle plane and  $\theta_x = K/\gamma$  in the particle oscillation plane. The  $\theta_x = K/\gamma$  dependence arises since  $\vec{p}$  is constantly changing its transverse component throughout the betatron orbit. When  $K \gg 1$ , only certain phases along the betatron trajectory will make a contribution to the observed spectrum in a direction of observation defined by  $\vec{k}$ . These phases correspond to the maximum positive and negative displacement regions of the electron trajectory where the acceleration is the greatest, and locally  $\vec{k}$  is parallel to  $\vec{p}$ . This allows for a "synchrotron-like" spectrum approximation for the photons, eliminating the resolution issues associated with spectral harmonics. This is the premise of the Saddle-Point Method solution for high-K wigglers [5].

A Fortran90 code has been written to compute the far-field spectrum of the plasma wiggler using the Saddle-Point Method. The result gives the energy per unit frequency per unit solid angle ( $\frac{d^2W}{d\omega d\Omega}$ ) in the far-field. Using the Simpsons 3/8 rule, the spectrum is integrated over  $d\Omega$  to get the total energy radiated per unit frequency. If integrated over frequency, we find the result from Eqn. (5). For the  $n_{pe} = 1 \times 10^{17} cm^{-3}$ ,  $n_{pe} = 2 \times 10^{17} cm^{-3}$ , and  $n_{pe} = 3 \times 10^{17} cm^{-3}$  cases, the simulated energy loss agreed with Eqn. (5) to within 0.0035, 0.0062, and 0.021, respectively. A large sum of the electron energy can be lost in a short distance in a high-K plasma wiggler. This is accounted for by adjusting  $\gamma$  after a certain percentage of energy loss.

For a beam of electrons, the user inputs a radial distribution ( $w_e(r)$ ) and a total number of electrons ( $n_e$ ) for the beam. The radiation ( $\frac{d^2W_r}{d\omega d\Omega}$ ) is computed for each betatron radius ( $r$ ) for all  $\vec{k}$  and multiplied by the total number of electrons in that radial bin, defined by  $\frac{d^2W_r}{d\omega d\Omega} \cdot w_e(r) \cdot n_e$ . This gives the total far-field spectrum for the x-z plane. Radiation is only computed in one quadrant since the beam is assumed to have azimuthal symmetry. This assumption is justified since the target and detectors also contain that symmetry. The azimuthal symmetry guarantees that all r-z

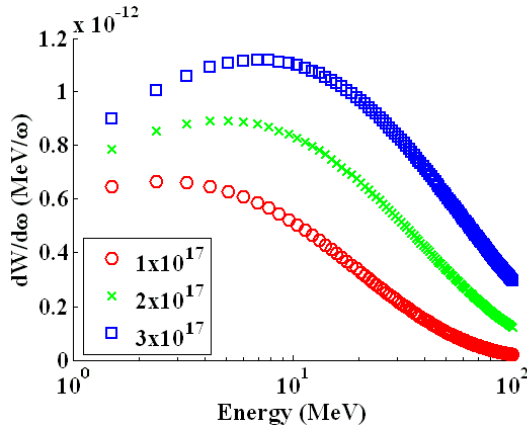


Figure 3: Calculated  $dW/d\omega$  for the collimated 8mm photon beam from a 28.5 GeV Gaussian beam at three different densities ( $cm^{-3}$ ). All cases assume  $L_p = 10cm$ ,  $\sigma_r = 10\mu m$ , and  $n_e = 9.6 \times 10^9$  where  $n_e$  is 60 percent of the incident electrons.

planes have equivalent spectra. Thus, the spectrum from the x-z plane is mirrored and added at all  $\phi$  points to simulate electrons in all r-z planes, decreasing the computational time. Figure 3 shows the calculated spectra for the 8mm beam at various densities.

It should be noted that an energy correction term needs to be added to the code for the bulk of electrons that contribute to the wake generation in the PWFA. Ideally, the bunch length should be longer to still allow for field ionization, but to eliminate large energy losses due to wake generation.

### Target Interaction/Particle Detection

EGS4 is used to calculate the positron yield. The input deck for EGS4 is created in the following way. The spectrum is calculated as defined above. Each quadrant is broken up into 15 areas. Within each area, the spectrum and total radiated energy are calculated, determining the photons/energy in each energy bin to be input into EGS4.

EGS4 calculates whether the positron will enter the magnet aperture. If so, the positron energy, position and direction cosines are sent to a particle tracking code written in MATLAB. Each positron is sent through the transfer matrix for our magnetic spectrometer. A count is recorded if the detector is hit.

## RESULTS

For the three cases shown in Figure 3, the spectra were sent through EGS4 with a  $.4X_o$  (1.42 cm) Ti target. This is known to be an optimal thickness [6]. The results were input into the particle tracker code. The positron spectra for the stigmatic plane of the magnetic spectrometer are shown in Figure 4. If integrated, we get absolute positron yields from 0-40 MeV of  $2.48 \times 10^6$ ,  $6.88 \times 10^6$ , and  $1.24 \times 10^7$  for the densities of  $n_{pe} = 1 \times 10^{17} cm^{-3}$ ,  $n_{pe} = 2 \times 10^{17} cm^{-3}$

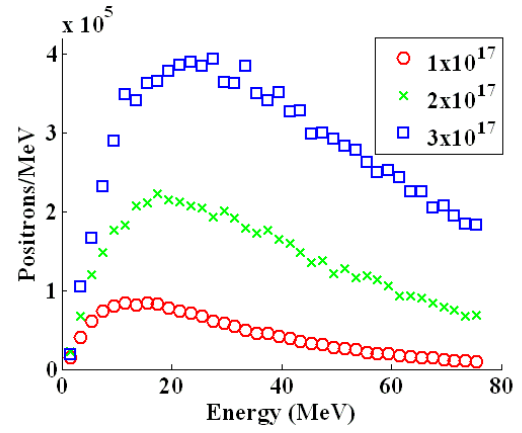


Figure 4: Simulated positron spectrum on detectors for cases in Figure 3 from the particle tracking code.

and  $n_{pe} = 3 \times 10^{17} cm^{-3}$ , respectively. As expected, the absolute positron yield is larger at higher densities.

These are the spectra we expect to detect in the experiment. However, we are only using about 4 percent of the available photon energy due to the beam collimation, and our plasma is a mere 10cm in length. Furthermore, the collection system would be optimized to collect the largest signal possible. These factors have a great effect on the absolute collected yield. An actual source design would supply orders of magnitude improvement in overall yield.

## CONCLUSION

A novel positron source could be achieved using the betatron radiation in a high K plasma wiggler. With the E-167 experimental densities, we can achieve focusing gradients of 9 MT/m with critical photon energies of approximately 50 MeV for on-axis radiation. A code has been developed using Fortran90, EGS4 and MATLAB to simulate the entire positron experiment. Photon spectra and yield have been calculated and presented. The spectral intensity of the plasma wiggler provides advantages that should not be overlooked. These numerical calculations will be compared to experiment in the E-167 experiments at SLAC.

## REFERENCES

- [1] E. Esarey et al., Phys. Rev. E, **65**:056505, 2002.
- [2] K. Flöttmann, *Conversion of Undulator Radiation*, edited by Chao and Tigner in *Handbook of Accelerator Physics and Engineering*. World Scientific Publishing Co. Pte. Ltd., 1998.
- [3] S. Wang et al., Phys. Rev. Lett., **88**:135004, 2002.
- [4] J.D. Jackson. *Classical Electrodynamics, 3rd Edition*. John Wiley and Sons, Inc., 1999.
- [5] I. Kostyukov et al., Phys. Plasmas, **10**:4818-4828, 2003.
- [6] K. Flöttmann, "Positron Source Options for Linear Colliders." 9th European Particle Accelerator Conf., 69-73, 2004.